

A METHOD OF SWITCH SELECTION FOR AN ELECTRIC VEHICLE DRIVE

D. A. Finn and G. R. Walker

School of Computer Science and Electrical Engineering
University of Queensland
dfinn@csee.uq.edu.au

Abstract

The key to reducing cost of electric vehicles is integration. All too often systems such as the motor, motor controller, batteries and vehicle chassis/body are considered as separate problems. The truth is that a lot of trade-offs can be made between these systems, causing an overall improvement in many areas including total cost.

Motor controller and battery cost have a relatively simple relationship; the less energy lost in the motor controller the less energy that has to be carried in the batteries, hence the lower the battery cost. A motor controller's cost is primarily influenced by the cost of the switches. This paper will therefore present a method of assessing the optimal switch selection on the premise that the optimal switch is the one that produces the lowest system cost, where system cost is the cost of batteries + switches.

1. INTRODUCTION

When selecting switches for any motor controller, the most common design strategy is to find the lowest cost switches that can process the power. In industrial applications this is often the optimal solution, but for electric vehicles (EVs) where energy is a valuable commodity a more holistic approach needs to be taken.

The major cost in electric vehicles is energy storage and generation, hence the high value placed on this commodity. Batteries, Super Capacitors, Fuel cells are all expensive items. The excessive cost of energy storage means that drive train efficiency must be as high as possible, so not to waste this precious resource. To do this both the drive train and energy source must be optimised as one system.

To be able to relate motor controller efficiency and energy storage cost, the power loss in the controller must be integrated over a typical model driving cycle. The lower the power loss of the controller, the less money that needs to be spent on batteries. Therefore, the price of interest is $\text{cost}(\text{Batteries}) + \text{cost}(\text{MotorController})$, the inputs needed to calculate this cost are shown in figure 1.

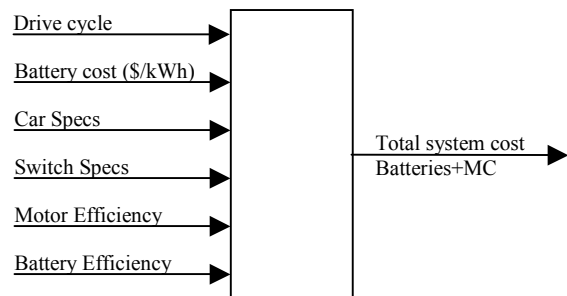


Figure 1 – Switch Evaluation System

2. DRIVE CYCLE

The drive cycle is an important input into the design process. For example, it allows MOSFETs to be a better choice in controllers where the power rating would usually dictate the use of IGBTs.

Two different drive cycles have been considered and assessed separately. The city cycle used is the Urban Dynamometer Driving Schedule (UDDS) that is 11.9km long. The highway cycle used is the Highway Fuel Economy Test (HFET) that is 16.4km. These two cycles are shown in figure 2 [1]. To give the EV a more realistic range these driving cycles have been multiplied by 10, giving the EV city range of 119km and a highway range of 164km.

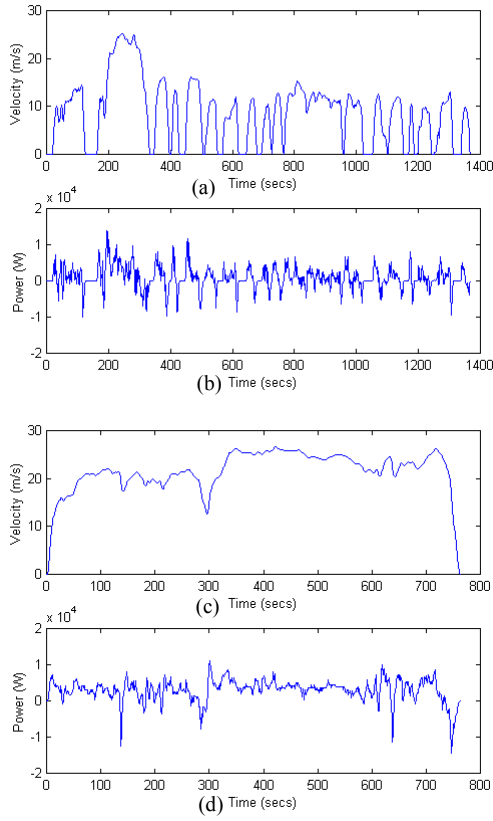


Figure 2 – (a) & (b) UDDS cycle, (c) & (d) HFET cycle.

To calculate the instantaneous power through the controller at any time during either of the mentioned cycles, equation (1) is used [2].

$$P(v) = \frac{1}{2} \rho C_d A v^3 + C_{rr} m g v + m \frac{dv}{dt} v + m g Z v \quad (1)$$

Mass of the car	m	630kg
Coefficient of air drag × Frontal Area	$C_d A$	$0.3m^2$
Coefficient of rolling resistance	C_{rr}	0.0075
Acceleration due to gravity	g	$9.8m/s^2$
Air Density	ρ	$1.17kg/m^3$
Wheel radius	r	0.3m

The gradient, Z, in equation (1) is assumed to be zero in both the UDDS and HFET driving cycle, hence power becomes purely a function of velocity. The output of this function can be seen in figure 2 parts (b)&(d).

Figure 2 parts (b)&(d) also give an indication of the power requirement to perform the driving cycle. A maximum power of approximately 15kW can be observed in figure 2, allowing for a safety margin, a 20kW controller will be assumed.

3. ASSUMPTIONS

Although this procedure could be applied to many different situations and applications, the procedure will be applied to a particular situation and the results presented.

Cost of the batteries is assumed to be \$700/kWh, this is in line with Andersson [3]. The drive cycle battery efficiency is assumed to be approximately 90% and the motor efficiency also assumed to be approximately 90%.

The controller is assumed to be a standard 6 switch 3 phase bridge. It uses standard 120° conduction and PWM control at a switching frequency (f) of 20kHz. The motor is assumed to be a standard brushless DC with a square wave backEMF. This is typical of the approach adopted by many of the Japanese manufactured EVs, such as the Toyota RAV-EV and Honda EVplus.

4. MOTOR CONTROLLER POWER LOSS

To calculate the power lost in the controller the RMS currents in each of the components must be found. To find these currents the following steps have been taken.

- The input voltage is assumed to be 75% of rated switch voltage

$$V_i = 0.75 V_{ds}$$

Industrial drives work with a 50% margin (1200V switches with 600V bus). With an integrated system design, 75% should be achievable.

- The output voltage can be calculated using the motor constant

$$V_o = \frac{V_i S}{S_{oMax}} \quad \text{where } S \text{ is motor speed} \\ S_{oMax} \text{ is rated speed}$$

- Motor current can be found from the output power and output voltage

$$I_m = \frac{P_o}{V_o}$$

- It has to be calculated whether the controller is in a continuous or discontinuous region of operation. If $t_{off} + t_{on} \geq T$ then the controller is in continuous operation otherwise it is in discontinuous operation. Where:

$$t_{on} = \sqrt{\frac{2TLI_m}{V_i \left(\frac{V_i}{V_o} - 1 \right)}}$$

$$t_{off} = \frac{(V_i - V_o) t_{on}}{V_o}$$

The RMS currents in the controller components are given by the equations in table 1.

Continuous conduction mode	Discontinuous conduction mode
$D = \frac{V_o}{V_i}$	$D = \frac{t_{on}}{T}$
$t_{on} = DT$	
$t_{off} = T - t_{on}$	
$i_L = t_{on} \frac{V_i - V_o}{L}$	$i_L = t_{on} \frac{V_i - V_o}{L}$
$i_{L\min} = I_m - \frac{1}{2} i_L$	$i_{L\min} = 0$
$i_{Lrms} = \sqrt{I_m^2 + \frac{1}{3} (\frac{1}{2} i_L)^2}$	$i_{Lrms} = i_L \sqrt{\frac{1}{3T} (t_{off} + t_{on})}$
$i_{hsrms} = \sqrt{D} i_{Lrms}$	$i_{hsrms} = \sqrt{\frac{1}{3} D} i_{Lrms}$
$i_{lsrms} = i_{Lrms}$	$i_{lsrms} = i_{Lrms}$
$i_{drms} = \sqrt{1 - D} i_{Lrms}$	$i_{drms} = i_L \sqrt{\frac{1}{3T} t_{off}}$
$i_{crms} = \frac{1}{2\sqrt{3}} i_L$	$i_{crms} = \frac{1}{2\sqrt{3}} i_L$

Table 1 – Equations for RMS current

Switch specifications are needed to calculate the power loss and the price of the controller. The following specifications are required.

- 1) Switch type (MOSFET\IGBT)
- 2) Switch Price
- 3) Maximum power out [P_{oMax}]
- 4) Maximum speed [S_{oMax}]
- 5) On switching time [T_{swon}]
- 6) Off switching time [T_{swoff}]
- 7) On state resistance (for MOSFETs) [R_{ds}]
- 8) On state voltage drop (for IGBTs) [$V_{ce(sat)}$]
- 9) Maximum switch voltage [V_{ds}]
- 10) Diode forward drop [V_f]
- 11) Diode current for rated reverse recovery charge [I_f]
- 12) Reverse recovery charge [Q_{rr}]
- 13) Number of switches in parallel [nrsw]

The power loss in each component is calculated using the specifications from above.

MOSFET conduction losses are again completely resistive. Given 120° conduction there is only ever one high side and one low side switch on at any one time.

$$P = \left(i_{hsrms}^2 + i_{lsrms}^2 \right) \frac{R_{ds}}{nrsw}$$

IGBT conduction losses are solely a voltage drop.

$$P = (i_{hsrms} + i_{lsrms}) V_{ce(sat)}$$

To calculate switching losses the following calculations are used to give approximate answers.

Figure 3 shows a simplified version of the switching waveform [4].

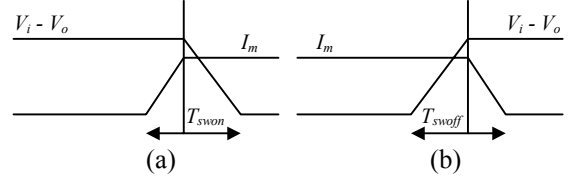


Figure 3 - Switching waveforms (a) on and (b) off.

Switch on losses:

$$P = \frac{1}{2} i_{L\min} (V_i - V_o) T_{swon} f$$

Switch off losses:

$$P = \frac{1}{2} (i_{L\min} + i_L) (V_i - V_o) T_{swoff} f$$

Diode conduction losses are again solely a voltage drop.

$$P = i_{dcon} V_f$$

Diode reverse recovery losses occur when the switch on the opposite side of the bridge leg switches on and current from the bus shoots through. This loss plays a fairly important role in shaping the power loss of MOSFET based controllers, because the MOSFET must rely on the intrinsic body diode to commutate the current and these diodes have a large reverse recovery charge.

$$P = \frac{Q_f}{I_f} i_{L\min} f V_i \quad [5]$$

All of the above power losses are added to give the power loss in the motor controller. This power loss when subtracted from the total power in, gives the power output. This output power divided by the input power gives the efficiency.

5. SWITCH SELECTION

The equations and procedures outlined in the previous section have been implemented as MATLAB code and the following switches considered.

Manufacture	Part number	Type	Price (AUD)
Infineon	SPW47N60C2	Single MOSFET	13
IXYS	IXFN180N20	Single MOSFET	114
IR	IRFP260N	Single MOSFET	8
IR	IRG4PC40UD	Single IGBT	13
IR	IRG4PC50UD	Single IGBT	20
IXYS	IXGH28N60B	Single IGBT	10
IXYS	MW1100-06A8	6 Pack IGBT	224
IR	GA150TS60U	Half Bridge IGBT	200

Table 2 – Considered switches [6],[7],[8].

The following two subsections demonstrate the importance of considering drive cycle and battery cost. Table 3 shows the ranked switches if they were to be chosen based on efficiency at rated power.

Part Nr	Efficiency
IRG4PC50UD	99.03
IRG4PC40UD	99
GA150TS60U	98.89
IXGH28N60B	98.87
MW1100-06A8	98.87
SPW47N60C2	98.29
IXFN180N20	96.12
IRFP260N	95.51

Table 3 – Ranking in terms efficiency

5.1 Efficiency contour plots

Efficiency contour plots for all of these switches have been generated; the four most interesting plots are shown in figure 4.

The SPW47N60C2 from Infineon that uses the new CoolMOS™ technology has quite a strange contour plot. It has broken the normal MOSFET trend where the R_{ds} increases exponentially with breakdown voltage, but still seems to follow the standard trend with respect to reverse recovery charge. The effects of shoot through losses due to this reverse recovery can be seen in the continuous conduction regions in the top left and right hand corners of figure 4(a).

The IXFN180N20 from IXYS is shown in figure 4(b), this plot shows predominately I^2R losses.

The IRG4PC40UD IGBT, from International Rectifier, shown in figure 4(c), has low on state losses as well low switching losses. The shoot-through losses are negligible due the fact that there is no intrinsic diode and hence the internal diode can be optimised for fast switching.

The MW1100-06A8, of figure 4(d), is an IGBT six pack from IXYS. Although the IGBTs in this package are standard technology the cost effectiveness of this type of IGBT is still good due to the packaging.

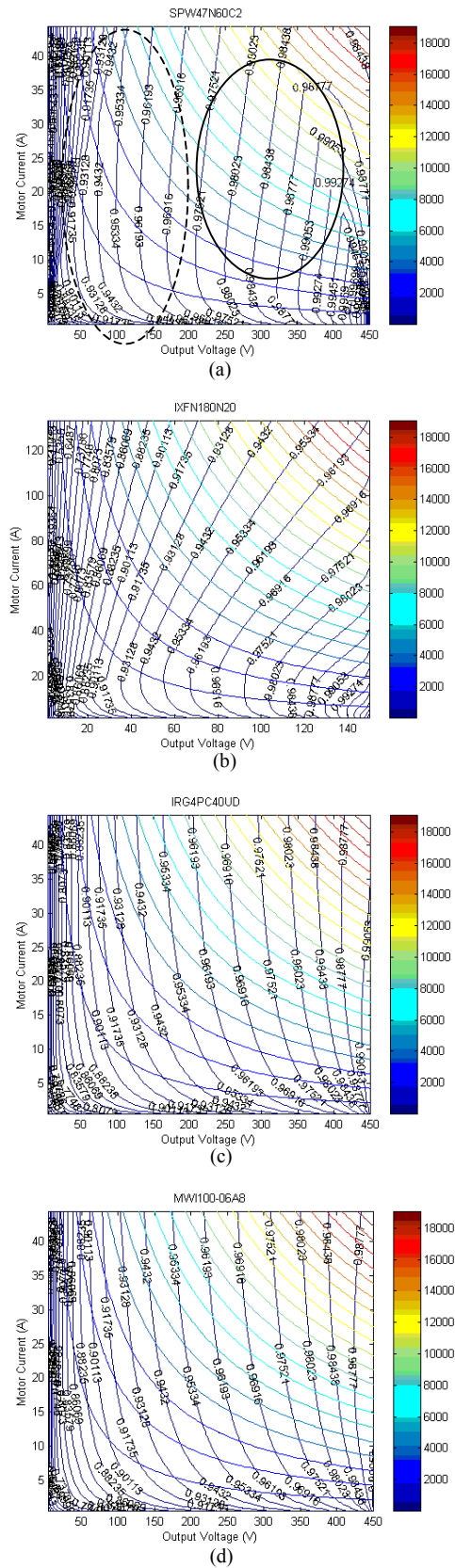


Figure 4 – Efficiency contour plots for selected switches in a hard-switched BLDC motor controller, (a) SPW47N60C2, (b) IXFN180N20, (c) IRG4PC40UD, (d) MW1100-06A8.

To give an indication of where most of the driving time is spent larger dashed ellipse, in figure 4(a), represents the city-driving region, while the smaller solid ellipse represents the highway-driving region.

5.2 Total system cost

The results of running the eight different switch options through both the city and highway cycles are shown, in order of best to worst value for money, in table 4. The first four options of table 4 are the same for both city and highway driving cycles and coincidentally are also ordered in terms of cycle efficiency. The other four options are quite unintuitive, for example, given the specifications of the IRFP260N it would have never even been considered as an option for a 20kW system. Yet it is cheaper than the IXFN180N20 by \$409 in the city and \$509 on the highway.

City Driving Cycle				
part nr.	eff	kWhbatt	mcprice	syscost
SPW47N60C2	92.04	5.56	234	4126
IRG4PC40UD	91.84	5.577	234	4138
MW1100-06A8	91.53	5.603	228	4150
IXGH28N60B	89.87	5.739	180	4198
IRG4PC50UD	91.76	5.584	360	4269
GA150TS60U	86.04	6.055	600	4838
IRFP260N	75.21	6.948	144	5007
IXFN180N20	76.79	6.817	684	5456
Highway Driving Cycle				
part nr.	eff	kWhbatt	mcprice	syscost
SPW47N60C2	97.5	8.027	234	5853
IXGH28N60B	95.09	8.216	180	5931
IRG4PC40UD	96.06	8.14	234	5932
MW1100-06A8	95.79	8.161	228	5941
IRFP260N	93.91	8.308	144	5960
IRG4PC50UD	96.02	8.143	360	6060
GA150TS60U	93.9	8.309	600	6416
IXFN180N20	94.31	8.277	684	6478

Table 4 – Ordered options for city and highway driving cycles

The cycle efficiency of table 4 is calculated by taking the total energy lost in the controller over the whole driving cycle, dividing it by the total energy used and taking that percentage away from 100%. So, the round trip efficiency of the controller is defined as

$$\eta = \left(1 - \frac{\text{energy lost to controller}}{\text{energy flow through controller}} \right) \times 100\%$$

The battery capacity of table 4 is calculated by adding all the energy loads:

- 1) driving the car (aerodynamic drag + rolling resistance)
- 2) motor (iron losses, copper losses)
- 3) motor controller (detailed above)
- 4) batteries (internal resistance losses, electrochemical losses)

The motor controller price listed in table 4 only takes into account the cost of the silicon, as the rest

of the motor controller cost is the same for all the listed options.

With the battery capacity known, the costs of batteries are easily calculated. Add to these battery costs the motor controller costs and the total system costs are obtained and shown in table 4.

6. CONCLUSION

A method for switch selection in EV motor controllers has been presented and demonstrated. The main conclusion that must be drawn from this paper is that, an EV motor controller must be designed in context. That is, the driving cycle and energy source cost must be taken into account.

7. REFERENCES

- [1] NREL, Advisor 3.1 Advanced Vehicle Simulator, Feb, 2001.
- [2] C. R. Kyle, Racing with the sun – The 1990 world solar challenge, Soc. of Automotive Engineers Inc, 1991.
- [3] B. Andersson, Battery Development for EVs, an update, EVS17, 2000.
- [4] Ned Mohan, Tore M. Undeland, William P. Robbins, Power Electronics : converters, applications, and design, J. Wiley, 1995, p584.
- [5] J.J.Sparkes, Semiconductor Devices, Chapman & Hall, 1994, p88.
- [6] Infineon, <http://www.infineon.com>, July, 2001.
- [7] IXYS, <http://www.ixys.com>, July, 2001.
- [8] International Rectifier, <http://www.irf.com>, July, 2001.